The Forcing of Antarctic Katabatic Winds

THOMAS R. PARISH AND KENNETH T. WAIGHT III

Department of Atmospheric Science, University of Wyoming, Laramie, WY 82071

(Manuscript received 3 June 1986, in final form 2 March 1987)

ABSTRACT

The temporal and spatial development of katabatic winds along an idealized slope representative of Antarctic terrain is examined using a hydrostatic, two-dimensional primitive equation model with explicit longwave radiation parameterization. A detailed diagnosis is made of a simulation in which katabatic flow develops from rest due to the strong radiational cooling of the underlying surface. Significant thermodynamic and dynamic differences are seen between the gravity-driven flows over the gently-sloping interior and over the steep ice slopes near the coast. The strongest temperature inversions and largest static stabilities are found over the interior of the continent, although the net cooling of the katabatic layer and magnitude of the downslope-directed horizontal pressure gradient force are greatest at the coast. The interior is characterized by low Rossby number, quasi-geostrophic type flows, while more intense, near-antitriptic winds occur at the coast. Model results are in reasonable agreement with the limited Antarctic observations.

1. Introduction

Katabatic winds have been perhaps the most celebrated climatic feature of Antarctica since the earliest expeditions onto the face of the continent. The literature is replete with documentation and testimonials of the early explorers regarding the intensity and persistence of the surface wind. The most striking narrative is from the Australasian Antarctic Expedition of 1911–14 which ventured to Cape Denison, along the coast of Adelie Land in East Antarctica (Fig. 1). The group's leader, Douglas Mawson, describes the katabatic characteristics in the popular account of the expedition *The Home of the Blizzard* (1915) noting that the katabatic stream was "a river, rather a torrent, of air [rushing] from the hinterland year after year, replenished from a source which never fails . . . ." The forcing of such flows can be traced to the strong cooling of air adjacent to the continental ice surface, producing a "sloped-inversion" pressure gradient force directed downslope. The gravity-driven component is by far the most significant factor in the surface wind regime. This is clearly demonstrated by the manned-station surface resultant wind statistics in Table 1. Antarctic winds display the highest directional constancy values (ratio of vector resultant wind magnitude to mean wind speed) on earth with values generally near or in excess of 0.80. The constancy of the wind, along with the close relationship between the wind direction and the orientation of the terrain, strongly emphasize the central role of topography in shaping the character of time-averaged flows. This topo-dynamic coupling is of practical significance to field researchers in Antarctica as well. The strongest sloped-inversion pressure gradients and, consequently, strongest slope flows occur under the most extreme temperature inversions. Wendler and Kodama (1984) note a strong correlation between wind speed and cold temperatures for their automatic weather stations D-10 and D-57 located in the near-coastal vicinity of Adelie Land.

While coastal katabatic winds have incited most historical and contemporary discussion from Antarctic scholars, similar though not nearly as intense slope flows may be traced well into the continental interior. As shown in Fig. 1, Antarctica is a massive dome of ice with a maximum interior elevation in excess of 4000 m. Most of the continent lies above 2000 m and approximately 30% above 3000 m. Terrain slopes over the interior areas are quite gentle, averaging perhaps 2×10^{-3}. Over the high plateau regions, the ice slopes are comparable to the Great Plains region of the United States. It is only along the 50 km or so of coastal stretch that terrain slopes reach 10^{-2}, increasing to nearly 10^{-1} near the coastline (Mather and Miller, 1966). In terms of areal extent, the much-heralded katabatic storms occur over a very small fraction of the continent. Resultant wind statistics for selected interior stations are also listed in Table 1.

The topic of Antarctic slope flows has been the subject of numerous studies. A number of different existing models attempt to simulate observed drainage flows. Previously, Parish (1982a) has used the simple Ball (1960) model to depict the time-averaged wintertime near-surface drainage streamlines over the interior of East Antarctica. In addition, Parish (1984) has employed a three-dimensional numerical model to explain the occurrence of the anomalously intense coastal katabatic regime at Adelie Land. Both studies have fo-

© 1987 American Meteorological Society

Unauthenticated | Downloaded 06/13/21 12:38 AM UTC

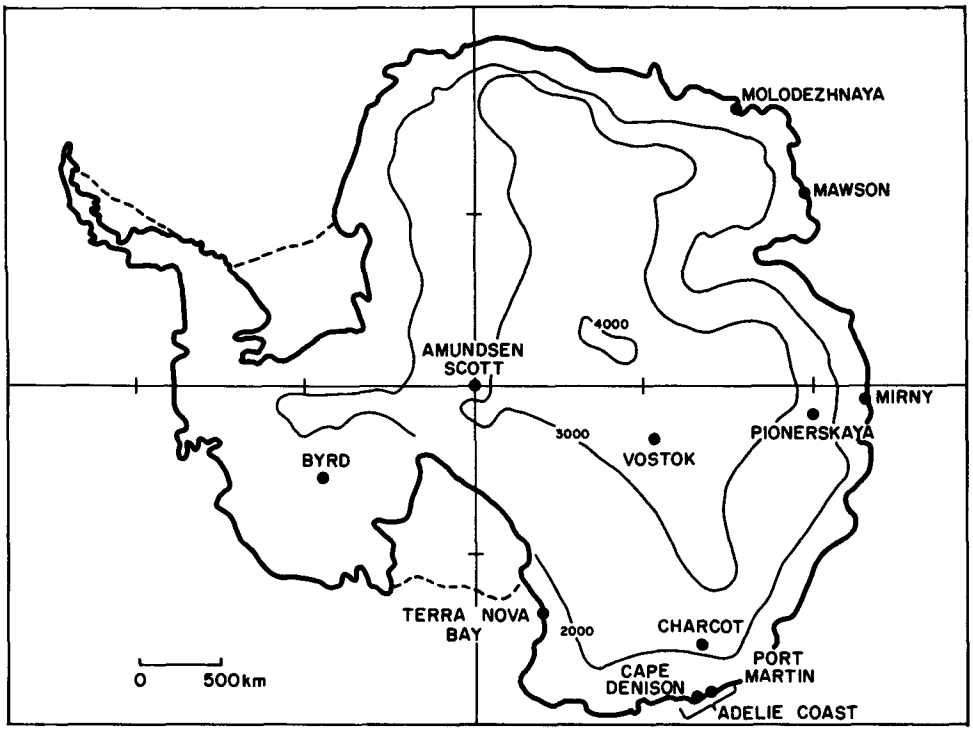

FIG. 1. The Antarctic continent including positions of stations mentioned in text. Contour lines drawn for 2000, 3000 and 4000 m only.

cused on the final, near-steady flow regimes. The purpose of the present paper is to 1) examine, in detail, the physical processes responsible for the temporal development of slope flows over the Antarctic continent; and 2) describe the complete ensemble of slope flow regimes which occur over the continent from the gently sloping interior to the steep coastal slopes. In particular, emphasis will be placed on the quantification of the adjustment process during the flow evolution. Terms in the horizontal scalar equations of motion and thermodynamic equation will be examined during the development of the drainage flows to isolate primary forcing mechanisms and to differentiate interior and coastal wind regimes.

TABLE 1. Mean yearly resultant wind statistics for stations in the interior and coastal regions of Antarctica. (N refers to the length of the data record in years; the deviation angle is the angle between the resultant wind and fall line of the ice terrain.)

	N	Resultant wind (m s^{-1}, deg)	Directional constancy	Deviation angle
Interior stations				
Pionerskaya	1	9.3, 131°	0.92	55°
Charcot	1	8.6, 163°	0.91	50°
Vostok	16	4.1, 243°	0.81	60°
Amundsen-Scott	16	4.6, 039°	0.79	50°
Byrd	14	6.6, 013°	0.86	60°
Coastal stations				
Cape Denison	2	19.0, 161°	0.97	20°
Port Martin	2	16.9, 146°	0.94	−5°
Mawson	15	9.8, 130°	0.93	10°
Mirny	17	9.7, 127°	0.90	50°
Molodezhnaya	11	8.4, 126°	0.85	10°

2. A model of katabatic winds

a. *Model equations*

Topography is the most influential factor in determining the behavior of Antarctic slope flows. To properly simulate the entire spectrum of gravity-driven flows from the gently sloping high interior to the steep coastal slopes, it is necessary to introduce a representative terrain profile of the Antarctic ice dome. In this study, the uniform ice profile along the 90°E meridian was used as a representative slice of East Antarctica. The power law fit to this section of Antarctica is

$$z_g(x) = 3922.2\left(1 - \frac{x}{1\times 10^6}\right)^{0.4112}, \qquad (1)$$

where $z_g(x)$ is the terrain height in meters at a distance x from the top of the plateau. A comparison of this idealized ice profile with the actual terrain as inferred from the Drewry (1983) map is shown in Fig. 2. The slopes of (1) are plotted in Fig. 2; gentle slopes are found over most of the interior with increasingly steep ice slopes in the coastal vicinity. The idealized terrain profile will be used in all analyses to follow.

Unauthenticated | Downloaded 06/13/21 12:38 AM UTC

The model framework used to simulate katabatic flow is the primitive equation system discussed in Parish (1982b). The model equations are written in modified σ-coordinates where the vertical coordinate is defined as

$$\sigma = \frac{p - p_t}{p_s - p_t} = \frac{p - p_t}{p^*}. \tag{2}$$

Here p_t refers to the pressure at the top of the model (set to 25 kPa) and p_s is the surface pressure. A value of 100 kPa has been assigned to sea level surface pressure. The flux forms of the horizontal equations are

$$\underbrace{\frac{\partial p^* u}{\partial t}}_{uA} = \underbrace{-\frac{\partial p^* uu}{\partial x} - \frac{\partial p^* u\dot{\sigma}}{\partial \sigma}}_{uA} \underbrace{- p^* \left[\frac{RT}{(p^* + p_t/\sigma)} \frac{\partial p^*}{\partial x} + \frac{\partial \phi}{\partial x}\right]}_{uB} + \underbrace{p^* fv}_{uC} + \underbrace{F_u + H_u}_{uD} \tag{3}$$

$$\underbrace{\frac{\partial p^* v}{\partial t}}_{vA} = \underbrace{-\frac{\partial p^* uv}{\partial x} - \frac{\partial p^* v\dot{\sigma}}{\partial \sigma}}_{vA} \underbrace{- p^* f(u - u_g)}_{vB} + \underbrace{F_v + H_v}_{vC}. \tag{4}$$

The geostrophic wind component u_g is set equal to zero in the model simulations in order to isolate the katabatic motions. The capital letters beneath the individual terms in the equations of motion are for identification purposes and will be used in the diagnostic analyses of katabatic winds to follow. The x-direction is taken down the fall line following the idealized ice profile from the interior to the coast. The terms F and H refer to friction and subgrid-scale horizontal diffusion processes, respectively. All other symbols have their usual meteorological meaning. The model thermodynamic equation is

$$\frac{\partial T}{\partial t} = -u\frac{\partial T}{\partial x} - \dot{\sigma}\frac{\partial T}{\partial \sigma} + \frac{RT\omega}{c_p(p^*\sigma + p_t)} + \frac{Q}{c_p} + F_t + H_t. \tag{5}$$

The terms F and H again refer to vertical and horizontal diffusion. The diabatic heating term Q is equal to the net radiative cooling rate since phase change processes are not simulated. The final prognostic equation is the continuity equation:

$$\frac{\partial p^*}{\partial t} = -\frac{\partial p^* u}{\partial x} - \frac{\partial p^* \dot{\sigma}}{\partial \sigma}. \tag{6}$$

To close the system, the hydrostatic equation is required:

$$\frac{\partial \phi}{\partial \ln(\sigma + p_t/p^*)} = -RT. \tag{7}$$

The equations are integrated using the conventional centered-in-time (leapfrog) method. A total of 26 horizontal grid points are used with a grid spacing of 50 km. The model domain incorporates a wide range of Antarctic ice topography from the high plateau about 1000 km into the interior of the continent to the coast and extends to the northern edge of the sea ice which is assumed to stretch some 300 km from the steep coastal escarpment. The vertical grid resolution is variable to allow the highest resolution in the boundary layer. The lowest level is approximately 11 m above ground level; the boundary layer resolution is approximately 60 m. A total of 15 vertical levels are contained within the model. The staggered grid structure described in Anthes and Warner (1978) is employed. All

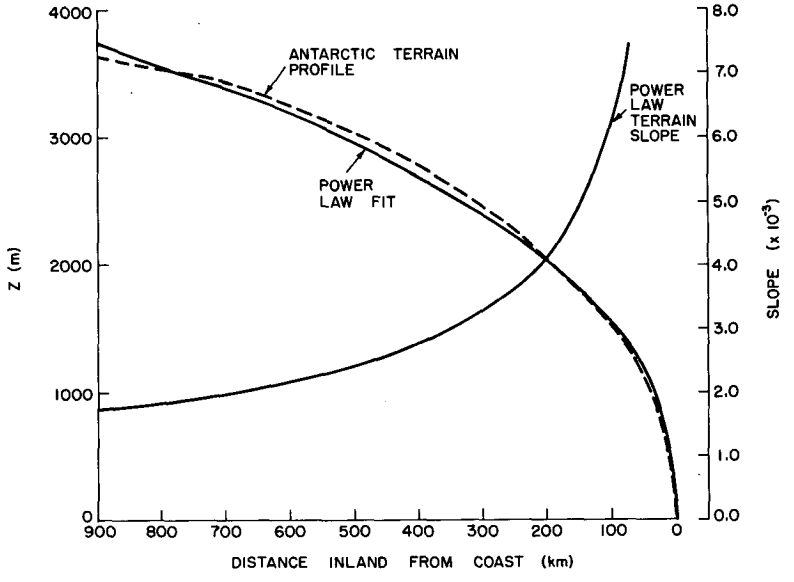

FIG. 2. Representative two-dimensional Antarctic terrain profile with power law fit.

Unauthenticated | Downloaded 06/13/21 12:38 AM UTC

prognostic variables are extrapolated outward to the boundaries as described in Parish (1982b).

b. Parameterization

By far the most important physical process during the development of katabatic winds is the radiational cooling of sloping ice terrain. Rather than adopt an arbitrary cooling rate to drive the slope flows, explicit longwave radiation is included in the model. The parameterization scheme is actually a graybody radiative transfer model based on recent estimates of the absorption characteristics of CO_2 and H_2O. Details of the radiation algorithm and verification of the radiative flux calculations can be found in Cerni and Parish (1984).

Turbulent fluxes of heat and momentum in the surface boundary layer (SBL) are modeled according to the similarity expressions of Businger et al. (1971). Above the SBL, the fluxes are computed using a first-order closure scheme where the eddy diffusivity coefficients are taken from the profile equation in Brost and Wyngaard (1978). The resulting K-value formulation compares favorably with actual eddy diffusivity estimates obtained from the micrometeorology tower data at Plateau station in the high interior of East Antarctica (see Kuhn et al., 1977).

The temperature at the ground is predicted from the force-restore slab model of Blackadar (1978). The surface energy budget equation is expressed as

$$\frac{\partial T_g}{\partial t} = C_g^{-1}\underbrace{(R_a - R_g}_{SA} \underbrace{- H_0)}_{SB} \underbrace{- K_r(T_g - T_m)}_{SC}, \qquad (8)$$

where R_a is the downwelling longwave radiation flux from the atmosphere, R_g the upward flux of radiation from the ice surface and H_0 the turbulent heat flux from the SBL. The parameter C_g is related to the thermal characteristics of the underlying terrain. For our purposes, C_g is set to 5.74×10^4 J m^{-2} K^{-1}. In this study, the relaxation coefficient K_r is set to 1.82×10^{-5} s^{-1} which corresponds to a periodic input of approximately 4 days. During austral winter with no incoming solar radiation, periodic changes in the surface temperature over the interior ice slopes are related to passage of cyclone systems in the vicinity of the coastline. Thick cloud shields as revealed on satellite imagery substantially increase the atmospheric downwelling radiation component, thereby acting to increase the temperature in the lowest portion of the atmosphere. The value of the relaxation coefficient represents the time scale associated with the cyclonic events as revealed in time series spectra such as in Mather and Miller (1966). As will be shown later, the time-evolution of the ground temperature is not particularly sensitive to the exact value of K_r. The term T_m is the mean temperature of the lowest layer, averaged over the time period associated with the passage of cyclonic events and is estimated from climatology.

3. Model results

a. Evolution of the state parameters

The basic katabatic simulation from which the diagnostic analyses are taken consists of a 24-h model time integration starting from conditions of rest. The initial ambient thermal structure was taken from the sounding information presented in Schwerdtfeger (1984; see his Fig. 6.9). The temperatures in the lowest levels of the atmosphere were extrapolated downward from the temperature profile above the inversion. Such conditions are assumed representative of pre-katabatic surges, where traveling cyclonic disturbances have recently disrupted the inversion structure and downslope gravity flows by substantial downward longwave radiation from thick clouds and/or mixing processes. The model simulation is made for clear skies and a relative humidity in the free atmosphere of 30%. As discussed in Cerni and Parish (1984), the relative importance of water vapor in the radiation scheme is strongly dependent on temperature. For the extremely cold temperatures found in Antarctica, the actual water vapor content is very low. Therefore, the model results are quite insensitive to the exact moisture profile over the range of temperatures in the simulation.

To depict the evolution of the slope flows, the wind components and temperatures at several grid locations have been closely monitored. Three grid points have been selected for comparison, the first point located along the steepest stretch near the coast, the second point some 400 km in the near interior where ice slopes are somewhat transitional between the steep coastal slopes and gentle interior terrain slopes, and the third point deep in the interior approximately 800 km from the coastline. The downslope flows at all locations develop within several hours of the model start although the coastal location displays a much more rapid response than the interior sites. Much of the flow evolution is completed by 12 h and by the end of the 24-h integration period, near-steady conditions prevail. The evolution of the wind components and temperatures at the lowest σ-level (corresponding to the top of the SBL) for the three locations is shown in Fig. 3. Clearly, the coastal katabatic wind develops most rapidly in response to the strong and sudden radiational cooling. The resulting profiles of wind and the horizontal pressure gradient after the 24-h model integration for the three locations are shown in Fig. 4. The strongest katabatic winds are found in the steep coastal vicinity. It should be pointed out that the simulation represents ideal conditions for the development of katabatic winds and, therefore, the modeled katabatic winds are somewhat stronger than the resultant wind at most coastal stations. The simulated winds decrease in speed inland in response to the decreasing ice terrain

Unauthenticated | Downloaded 06/13/21 12:38 AM UTC

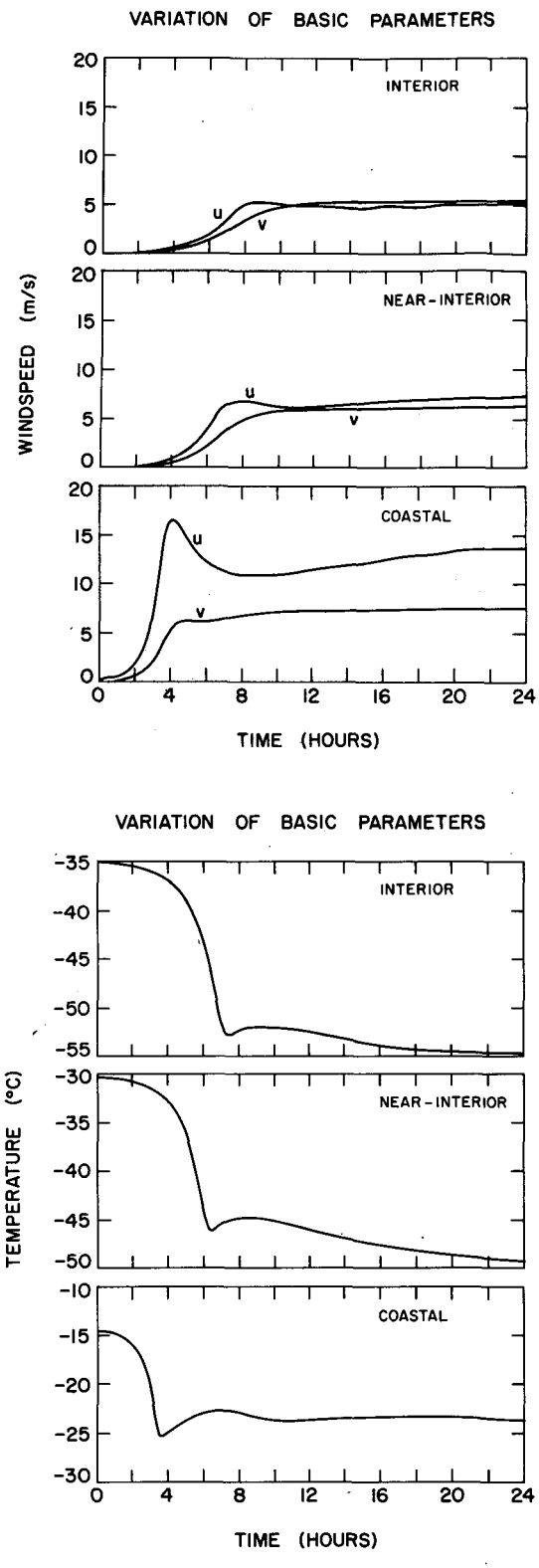

FIG. 3. Evolution of the horizontal wind components and temperature at the lowest σ-level during the 24-h model simulation. The u-component is taken to be in the positive x-direction (down fall line), and the v-component is taken to be in the positive y-direction (along terrain contours, to the left of u).

slopes. In addition, the deviation angle of the surface wind from the fall line increases with distance from the coastline. By approximately 400 km inland, the flow direction is more contour-parallel than downslope. This simulated feature of the wind is in good agreement with observed wind characteristics as revealed in Table 1. Specification of the boundary layer turbulent flux parameterization may introduce some uncertainty, but there is no reason to question the gross features of the katabatic wind. The profiles of the wind components for the near-interior point are representative of soundings shown in Adachi (1984) for Mizuho Station, located in the near-interior region of East Antarctica about 45°E at an elevation of 2230 m.

Also illustrated in Fig. 4 is the height variation of the y-component of the geostrophic wind (which corresponds to the sloped-inversion pressure gradient force) after the 24-h model integration period. The outstanding feature is the dramatic decrease of the geostrophic wind in the first few hundred meters above ground level. This effect is especially pronounced over the steep coastal slopes where a near-exponential decrease of the horizontal pressure gradient force is present in the lowest 300 m. As is to be expected, the strongest sloped-inversion pressure gradient force is observed at the lowest σ-level throughout the model domain and the largest values are associated with the steepest slopes. This characteristic decrease in the geostrophic wind with height emphasizes the importance of a realistic treatment of diabatic cooling processes and the interaction of the radiative cooling and turbulent heat exchange near the surface. The ability to resolve the vertical structure of such processes is a major advantage of a primitive equation model.

Significant modification of the low-level thermal structures takes place during the development of katabatic winds over the Antarctic ice surface. The low-level stability is enhanced over the entire continent with the strongest stability found over the gently sloping interior. Strong coastal katabatic winds effectively mix the lower atmosphere, resulting in weaker static stabilities over the continental periphery. At the start of the model integration period, potential temperature surfaces are aligned in a horizontal fashion since geostrophic winds in the free atmosphere are assumed to be zero. The isentropic surfaces quickly move upwards and become oriented in a direction parallel to the ice terrain as the model integration proceeds. By 24 hours, the isentropes are directed nearly parallel to the ice profile, being packed more tightly above the continental interior. The initial and near-steady 24 hour isentropic cross sections are illustrated in Fig. 5. Notice that nearly adiabatic temperature profiles are found along the ice surface by 24 hours. This feature has been reported by Radok (1973) based on temperature measurements along the surface of the Antarctic ice sheet and is thought to be representative of well-developed drainage flows.

Unauthenticated | Downloaded 06/13/21 12:38 AM UTC

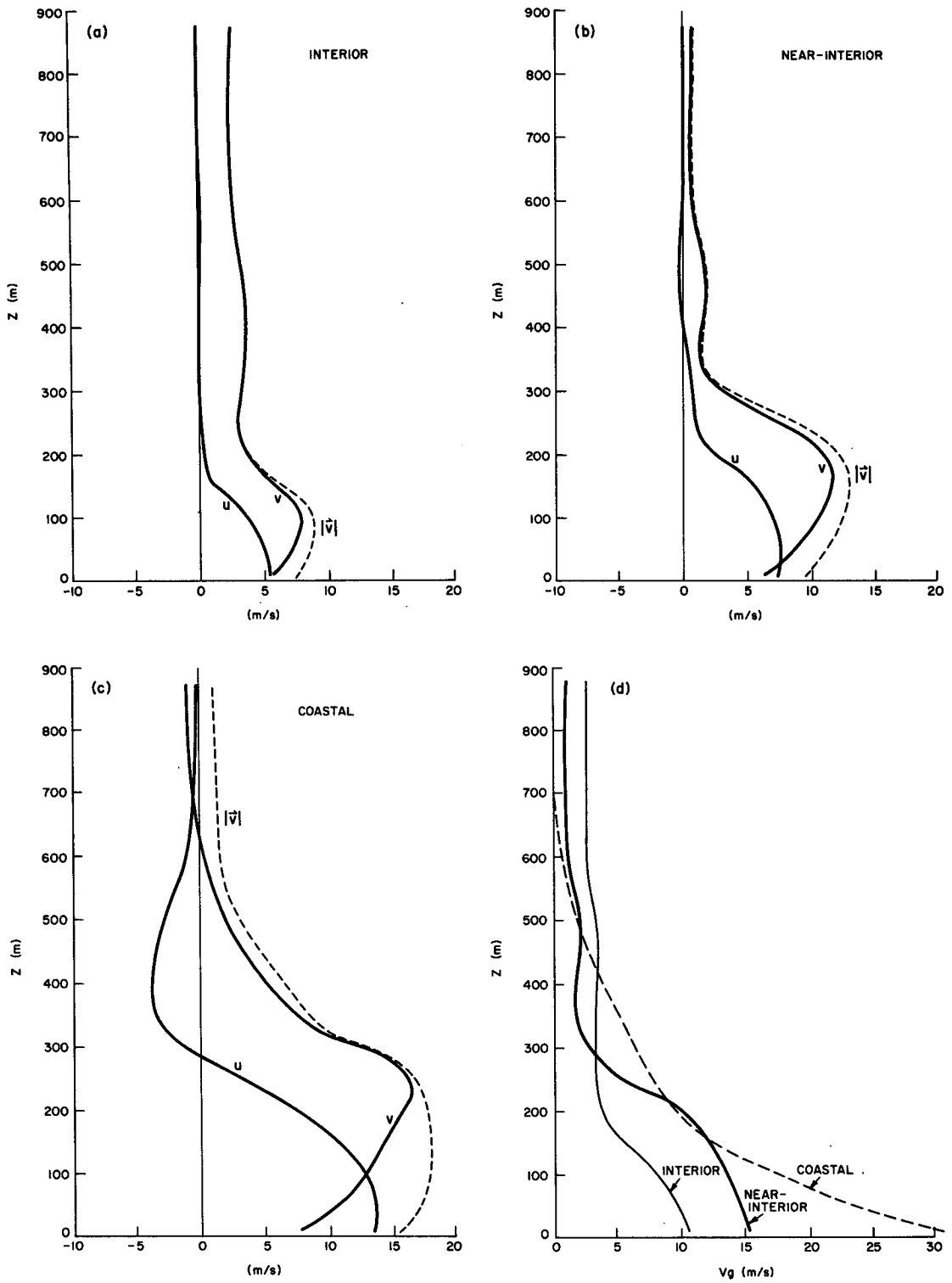

FIG. 4. Final vertical profiles of u, v and the magnitude of the horizontal wind vector (V) for (a) interior, (b) near-interior, and (c) coastal location. The final vertical profile of the y-component of the geostrophic wind is given in (d) for the three locations.

Unauthenticated | Downloaded 06/13/21 12:38 AM UTC

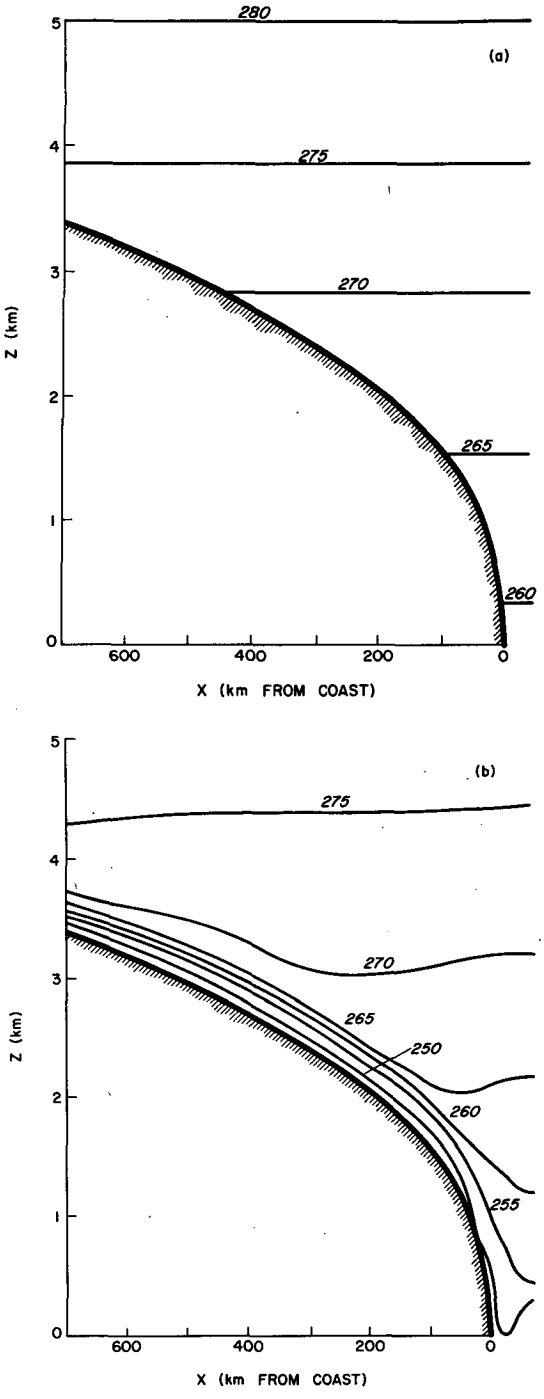

FIG. 5. The (a) initial and (b) final potential temperature (K) cross sections.

Details of the temperature and potential temperature profiles for the coastal, near-interior and interior sites after the 24-h integration period are shown in Figs. 6a and 6b. The simulated temperature inversions over the near-interior and interior are representative of actual profiles. For example, Pionerskaya is located in the near-interior region of East Antarctica at an elevation of approximately 2700 m with a terrain slope estimated to be 2.5×10^{-3}. Wintertime inversion strengths are commonly observed to be 10–15 K. The near-interior grid location is situated along the model ice terrain in nearly an identical location with an elevation of 2700 m and a local ice terrain slope of 2.7×10^{-3}. The simulated inversion strengths of approximately 17 K are consistent with observed values. Likewise, the nearly 20 K temperature inversion produced during the 24-hour model integration at the interior site is in reasonable agreement with inversions reported at stations deep in the interior of the continent such as Vostok. The coastal profiles suggest only weak inversions are present, a result confirmed by sounding data from the coastal station Mirny (Schwerdtfeger, 1970). In addition, the isothermal layer revealed above the boundary layer and extending perhaps 1000 m above ground level at the coastal grid location matches observed features (for example, Fig. 13 in Schwerdtfeger, 1970).

The profile of the 24-h potential temperature deficit from ambient conditions is shown in Fig. 6c. In general, the largest deficit occurs in the lower atmosphere over the more gentle slopes; the coastal katabatic winds effectively mix a deeper atmospheric column, thereby spreading the diabatic cooling throughout the lowest 1000 m.

b. *Diagnostic analyses of the forcing of katabatic winds*

The importance of the katabatic circulation on the energy budget of the Antarctic atmosphere is not known with any certainty. Without question, katabatic winds are a potentially large source of mass transport northward and may represent a significant sensible heat flux in the heat budget of the entire Southern Hemisphere. As a means of estimating certain bulk properties within the katabatic layer, a number of integral quantities have been defined,

$$\left.\begin{aligned} M &= \int_0^H \rho u\,dz, & P &= \int_0^H f v_g\,dz, \\ R &= (R_H - R_0) - H_0, & S &= \int_0^H \rho c_p u T'\,dz, \end{aligned}\right\} \quad (9)$$

where M is the downslope mass transport resulting from the katabatic flow, P the katabatic potential representing the integral of the sloped-inversion pressure gradient force over the depth of the katabatic layer with units of specific energy. Following Manins and Sawford (1979a), the net cooling rate of the katabatic layer, R, is just the sum of the radiative flux divergence over the katabatic layer ($R_H - R_0$) and the turbulent heat flux H_0 within the SBL. The horizontal flux of sensible heat per unit breadth across the katabatic flow is represented by S, where T' is the temperature deficit from ambient conditions. The upper limit H in the integral represents the seventh σ-level in the model (approximately 500

Unauthenticated | Downloaded 06/13/21 12:38 AM UTC

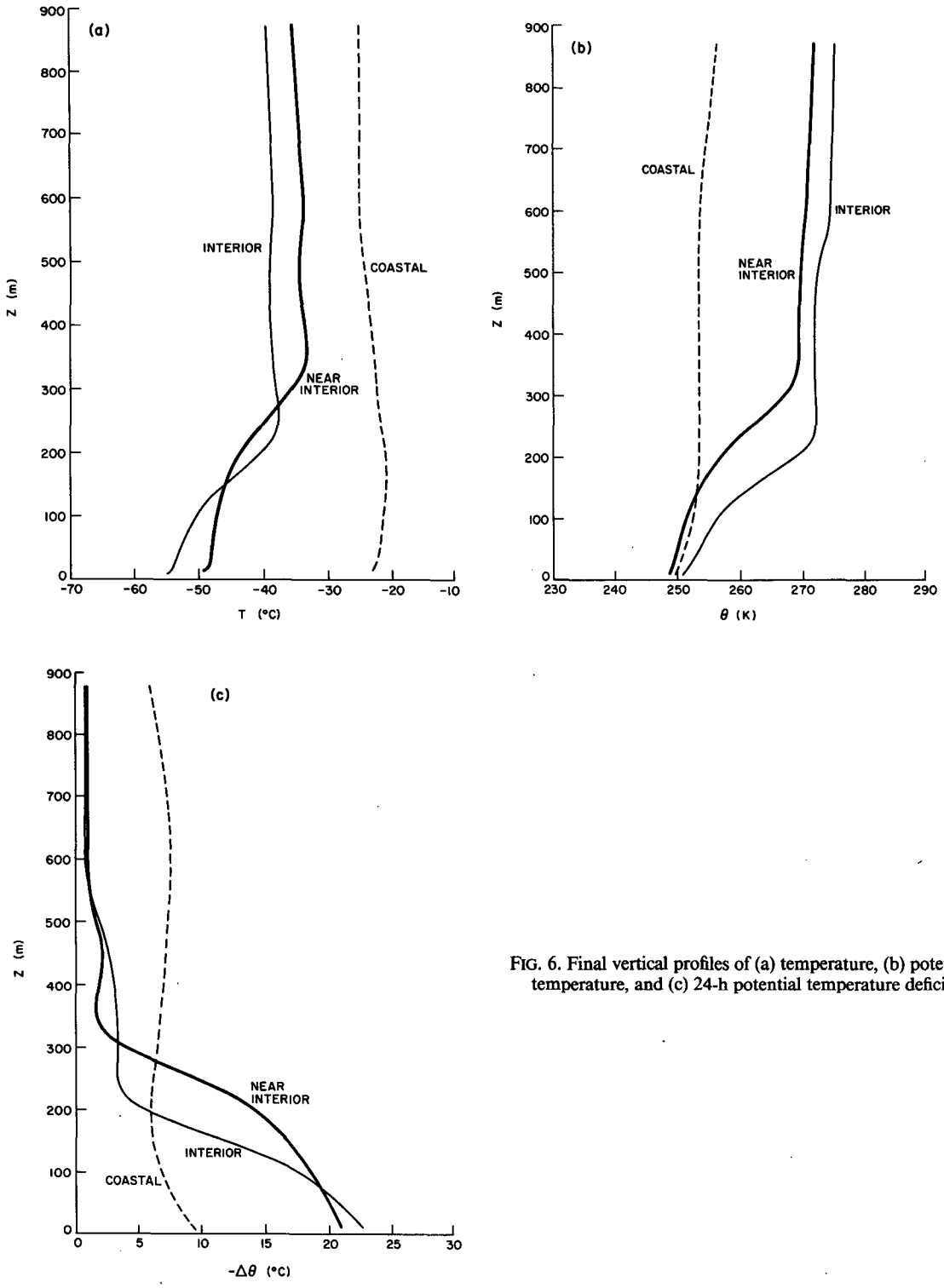

FIG. 6. Final vertical profiles of (a) temperature, (b) potential temperature, and (c) 24-h potential temperature deficit.

m above the surface) and is above the boundary layer for all points along the ice slope. Therefore, turbulent fluxes of heat and momentum are negligible at this level.

Variations of these integral quantities within the katabatic layer after the 24-h integration are shown in Fig. 7. Both the mass transport and katabatic potential (Fig. 7a) are sensitive to the terrain slopes and largest

Unauthenticated | Downloaded 06/13/21 12:38 AM UTC

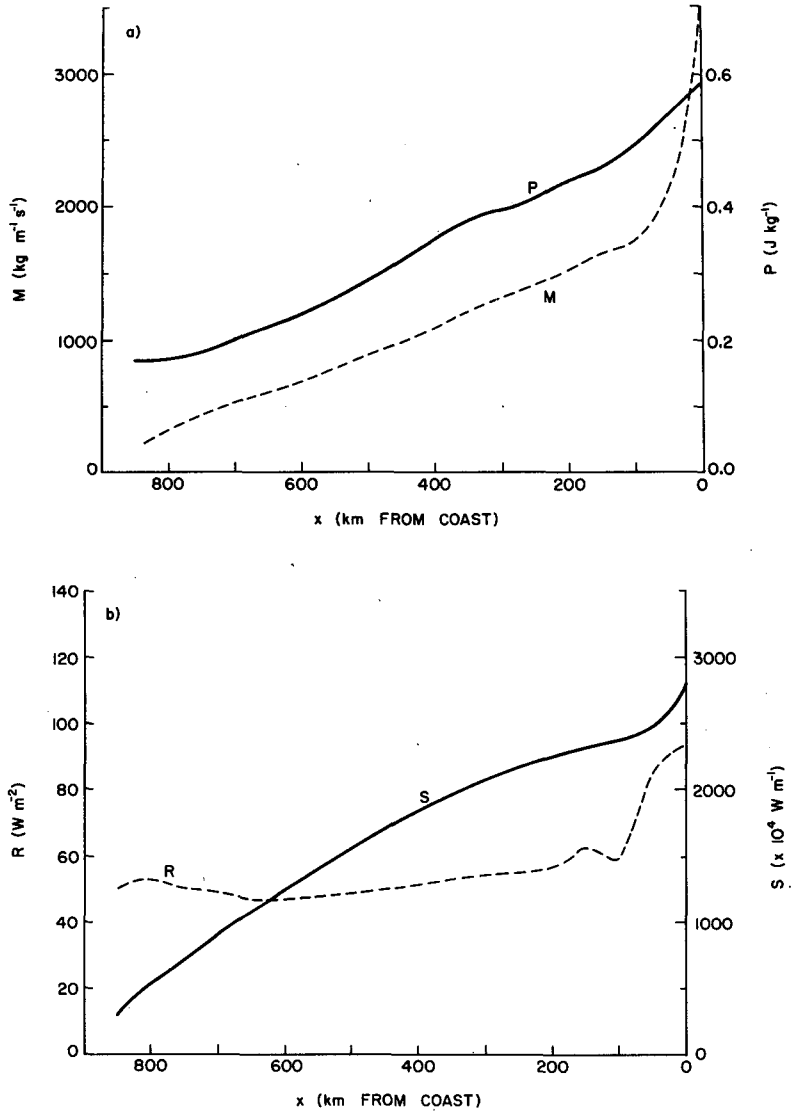

FIG. 7. Variation with distance along the slope of the final values of (a) mass transport (M) and katabatic potential (P), and (b) net cooling of the katabatic layer (R) and sensible heat transport (S).

values are found near the coast. The gradual increase in the mass transport observed towards the coast implies air in the free atmosphere must be entrained into the katabatic layer. This entrainment process acts to retard the katabatic winds in two ways. First, the air in the free atmosphere has little or no downslope-directed momentum and thereby acts as a drag on the katabatic layer when entrained. Second, the free atmosphere is relatively warm. Entrainment of this warmer air into the radiatively cooled katabatic layer acts to reduce the negative buoyancy and hence the sloped-inversion pressure gradient force. Over the interior of the continent, this entrainment velocity amounts to approximately 2×10^{-3} m s^{-1}. The strong increase in mass transport in the coastal vicinity requires an enhanced entrainment component which reaches 2×10^{-2} m s^{-1} at the terminal coastal grid point.

Turbulent entrainment at the top of the katabatic layer has been a topic of discussion in recent works pertaining to slope winds. As noted by Manins and Sawford (1979b), such entrainment is representative of an internal mixing process arising as the local Richardson number becomes subcritical. Manins and Sawford (1979a) suggest such entrainment may be the dominant retarding mechanism for katabatic winds. The Brost and Wyngaard (1978) K-parameterization used in the model is an explicit scheme and therefore is not designed to simulate such local mixing processes. However, the resulting Richardson numbers above the

Unauthenticated | Downloaded 06/13/21 12:38 AM UTC

ice slopes for the model simulation are generally well above the critical Richardson number of 0.25 except in the near-coastal vicinity where values within the katabatic stream are subcritical. This suggests that the mixing associated with the explicit K-parameterization appears to yield reasonable profiles of wind and temperature. An alternative scheme currently being explored is the local approach of calculating eddy viscosity values as discussed in Blackadar (1978).

A second type of entrainment can arise from mass divergence in the katabatic stream resulting from thermodynamic or dynamic differences along the slope. Continuity considerations dictate that a vertical velocity will then be induced in the ambient air. This is unrelated to turbulent entrainment, but will have similar consequences for the flow. We believe that this entrainment mechanism may at times be comparable in importance to the turbulent mechanism, especially in the near-coastal environment where terrain slopes increase rapidly towards the coast.

Figure 7b illustrates the net cooling rate and sensible heat flux within the katabatic layer. Notice that the net cooling rate shows only minor variation over the interior of the domain with representative cooling rates of approximately 50 W m^{-2}. The net cooling rate of the entire katabatic layer increases sharply near the coast in response to steeper slopes and stronger winds. This suggests that the net cooling rate of slope flows is dependent on the terrain slope and attendant wind regime and the assumption of a constant cooling rate in time and space may be unduly restrictive. The sensible heat flux shows a near-linear trend throughout the domain, increasing toward the coast. This implies that the increase in katabatic wind speed near the coast more than compensates for the decrease in the temperature deficit observed over the steeply sloping locations. It is difficult to generalize as to the importance of this sensible heat flux. The simulated katabatic flow occurs under ideal radiative conditions without influence of clouds or embedded drift snow. Certainly such conditions do not prevail over the entire continental periphery. In addition, significant variations in the intensity of katabatic winds are found along the coast (Parish, 1984).

To understand the evolution of the katabatic wind over the ice slopes of Antarctica, it is necessary to isolate the forcing mechanisms. In pursuit of this goal, the net diabatic cooling rate of the katabatic layer obtained from the thermodynamic equation and terms in the scalar equations of motion have been monitored throughout the katabatic wind development at the coastal, near-interior and interior locations. Ultimately, the radiative flux divergence at the surface is the driving mechanism for katabatic flow. The cooling of the air over the sloping ice terrain sets up a sloped-inversion pressure gradient force, acting to accelerate the low-level air in a downslope direction. A steady thermodynamic state at the surface is achieved when the net radiative fluxes directed away from the surface are balanced by the turbulent heat flux downward from the atmosphere and the conduction of heat through the ice. The time-evolution of terms in the surface energy budget for the coastal and near-interior grid locations are illustrated in Fig. 8. The net longwave radiation is initially the dominant forcing term, acting to cool the surface of the ice slope. The turbulent heat flux and katabatic wind are highly interactive. As the katabatic winds develop, the mixing processes become enhanced and the turbulent heat flux to the surface increases. This efficient removal of heat from the lowest levels of the atmosphere produces the sloped-inversion pressure gradient force and leads to the further enhancement of katabatic winds. The coupling between the turbulent

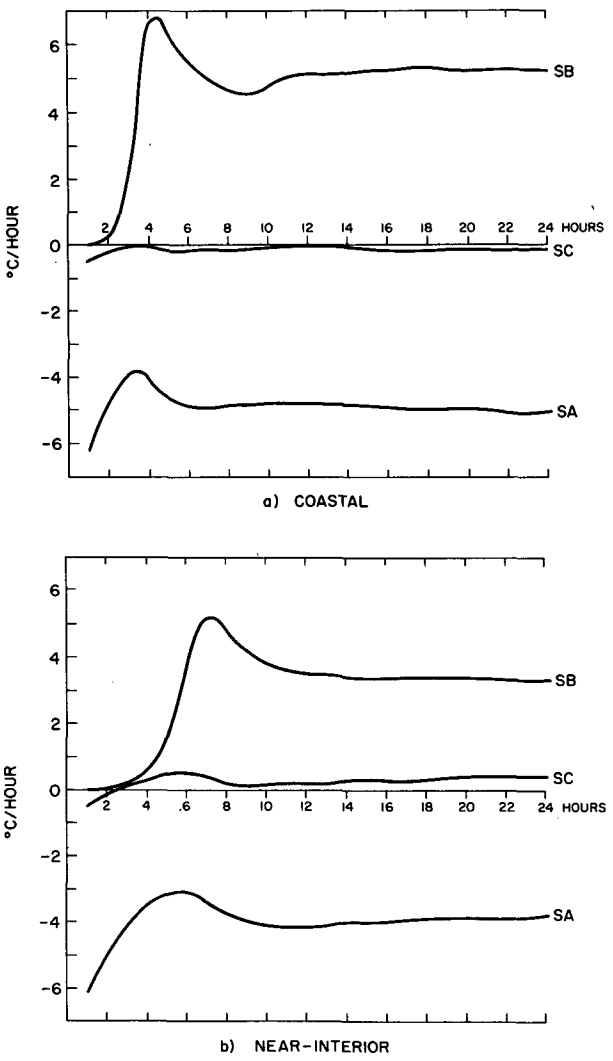

FIG. 8. Evolution of the terms in the surface energy budget for (a) coastal and (b) near-interior locations. The terms are labeled in (8) and are *SA*—net radiative flux, *SB*—turbulent heat flux, and *SC*—subsurface heat flux.

Unauthenticated | Downloaded 06/13/21 12:38 AM UTC

heat flux and katabatic wind can be seen by comparing Figs. 3 and 8. The turbulent heat flux is observed to be considerably larger over the steep coastal slopes than over interior locations in response to greater wind speeds. In addition, the turbulent heat flux shows a more rapid increase during the first few hours of katabatic wind development over the coastal slopes. Note that throughout the 24-h integration, the subsurface heat flux from the Blackadar (1978) expression is small.

The evolution of the net cooling rate of the katabatic layer over the ice topography is illustrated in Fig. 9. The cooling rate closely follows the katabatic wind development, suggesting that the turbulent flux of heat is far more efficient than radiational processes in cooling the atmosphere. The near-steady cooling rates are dominated by the turbulent flux component. At the coast, for example, the turbulent flux cooling rate of the katabatic layer amounts to approximately 80 W m^{-2}. The radiative cooling component is less than 10 W m^{-2} and subsoil conduction of heat (downward from the surface at the coast) approximately 2 W m^{-2}. This katabatic layer cooling rate is seen to depend significantly on the ice slope and stage of evolution of the wind.

During the course of katabatic wind development, strong interaction between the thermodynamics and dynamics takes place. The response of the terms in the horizontal scalar equations of motion at the coastal, near-interior and interior locations at the lowest σ-level is depicted in Fig. 10. The horizontal pressure gradient force (term uB) shows a rapid growth during the initial stages of the integration period, with the most dramatic increase at the coastal location. Also, the pressure gradient force displays a more rapid development for the steeper slopes. Note the initial peak associated with katabatic wind development occurs at approximately 3.6 h for the coastal locations, 6.4 h for the near-interior point and 7.4 hours for the interior site. Differences in the near-steady magnitudes of the pressure gradient force are apparent from Fig. 10 as well. Term uB is nearly three times as large at the coast as in the interior. The balance of forces in the later stages of the model integration period also point out fundamental differences in the Antarctic surface flow regimes. Near the coast, friction (term uD) is substantially larger than the Coriolis force (term uC). Thus, the coastal flows display antitriptic tendencies and the katabatic winds have a large downslope component. Note also that the horizontal and vertical advection terms (uA) are comparable to the Coriolis force. The Rossby number (ratio of the horizontal advection component to the Coriolis force) for the coastal katabatic flow is approximately 1.0 The balance of forces abruptly changes inland from the coast. The Coriolis force increases in relative importance, reaching the magnitude of the friction force. Owing to this change in the force balance, the slope flows in the interior are characterized by increasingly large deviation angles from the fall line as the terrain slopes decrease. The Rossby number is generally quite small; at the near-interior point Ro = 0.15 and at the interior location Ro = 0.08.

The evolution of the terms in the v-equation of motion (parallel to the height contours) is shown in Fig. 11. Unlike previous examples, little difference is observed over the widely varying terrain slopes. In all cases, a balance is reached between the horizontal pressure gradient–Coriolis force (term vB) and friction (term vC). Advection (term vA) is small in each case. The only differences are seen in the time of development of the ageostrophic accelerations and the magnitude, both of which are coupled to the downslope components of flow.

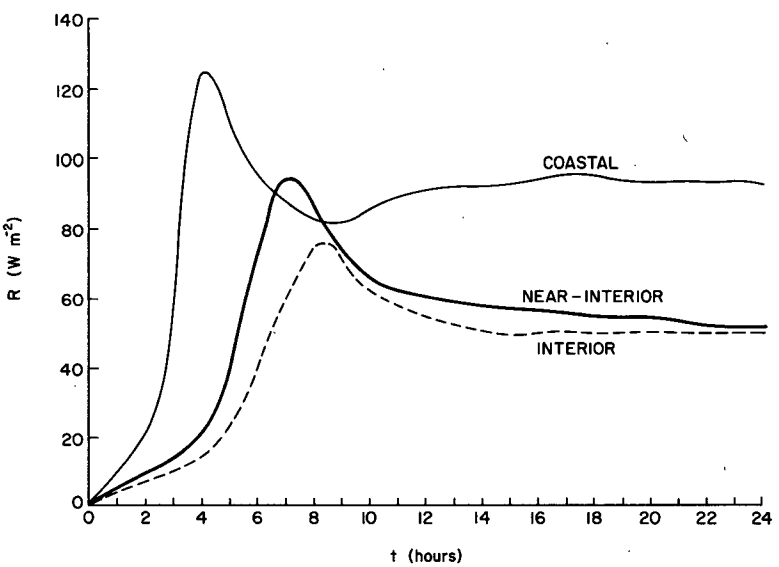

FIG. 9. Variation with time of the net cooling of the katabatic layer for the three locations.

Unauthenticated | Downloaded 06/13/21 12:38 AM UTC

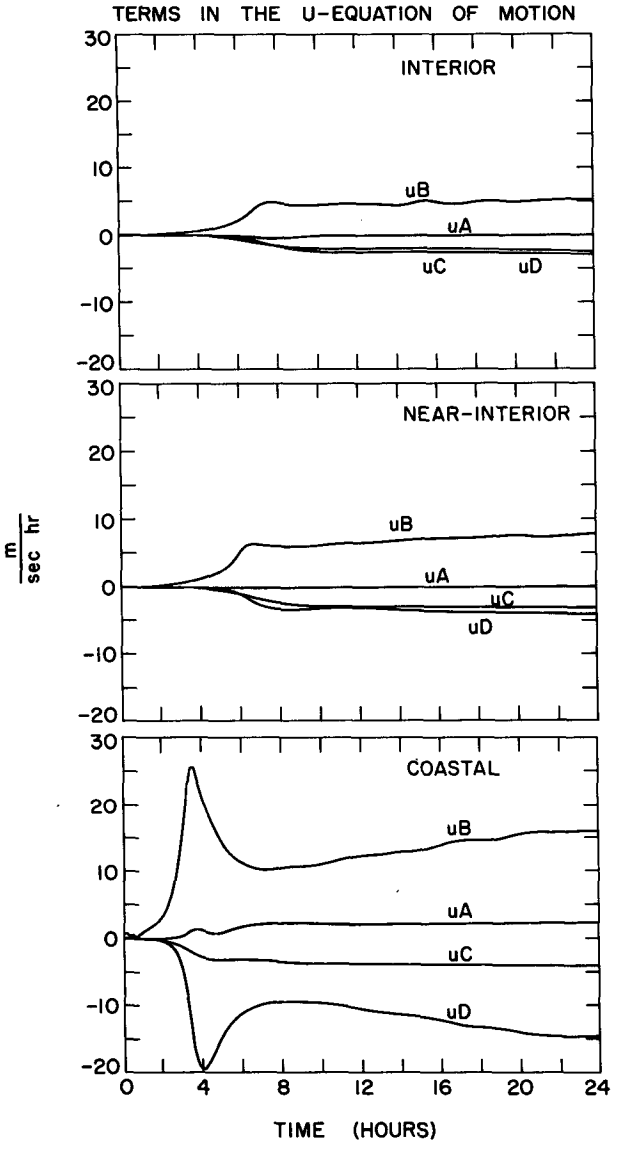

FIG. 10. Evolution of the terms in the u-equation of motion at the lowest σ-level. The terms are labeled in (3) and are uA—net advection, uB—pressure gradient force, uC—Coriolis force, and uD—vertical and horizontal diffusion.

4. Implications and conclusions

Antarctic katabatic winds are strongly controlled by the steepness of the ice terrain. It is not surprising, therefore, that significant dynamic and thermodynamic differences exist along a stretch from the gently sloping Antarctic interior to the steep coastal escarpment, since terrain slopes along this section vary in excess of one order of magnitude. As shown previously, katabatic winds at the coast are much stronger, directed more downslope and develop more abruptly than corresponding interior flows.

The horizontal pressure gradient created by the radiational cooling over the sloping terrain shows a marked difference between coastal and interior environments as well. The pressure gradient force is established much more quickly at the coast, reaching a peak magnitude over five times that found at the lowest level over the gentle interior slopes. The near-steady model wind regime at the coast suggests a quasi-antitriptic state in the lower atmosphere where the pressure gradient and friction forces are the largest terms in the x-equation of motion. Coriolis influences are of lesser importance, and scale with the horizontal advection of momentum. Interior flows by 24 h, on the other hand, show evidence of increasing importance of the Coriolis force which reaches a magnitude comparable to or exceeding the friction force. Interior near-surface slope

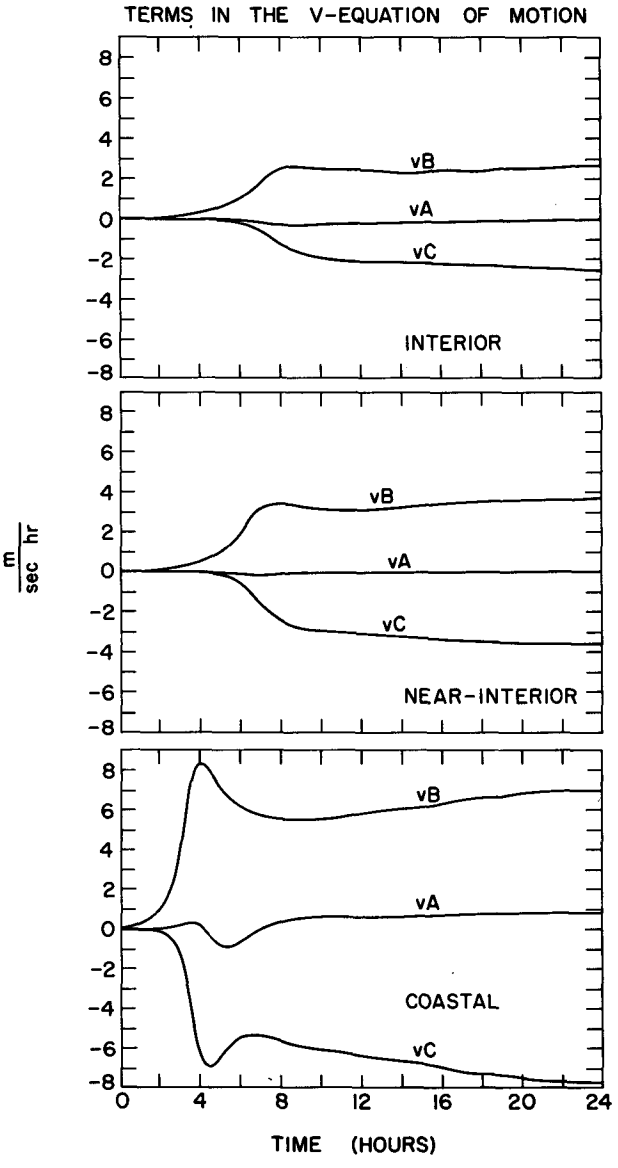

FIG. 11. Evolution of the terms in the v-equation of motion at the lowest σ-level. The terms are labeled in (4) and are vA—net advection, vB—pressure gradient—Coriolis force, and vC—vertical and horizontal diffusion.

Unauthenticated | Downloaded 06/13/21 12:38 AM UTC

flows are inherently low Rossby number, quasi-geostrophic phenomena. The steady nature of the slope flows over the interior of Antarctica lends itself to simple models such as that proposed by Ball (1960). The success of the time-averaged simulations of interior drainage flows (Parish, 1982a) is evidence of the relative simplicity of the force balance occurring over the Antarctic hinterland. Coastal slope flows are inherently more complex since the inertia terms become significant and the turbulent exchange processes are critical in the evolution of the katabatic wind. In addition, continuity effects become increasingly important since the downslope wind components increase significantly as the terrain slopes steepen. This suggests that a more detailed numerical approach is needed to properly simulate physical processes in the coastal environment.

These kinematic and dynamic differences have led some Antarctic scholars to question the generic use of the term "katabatic" to describe Antarctic slope flows. Schwerdtfeger (1970) notes that interior winds generally persist over much longer time periods than coastal flows because of the sensitivity of high wind episodes at the coast to upslope supplies of cold air and disrupting influences of cyclones. He uses the term "inversion" wind to differentiate the interior wind regime from the more intense coastal "katabatic" regime. This dichotomy in Antarctic slope flows is also discussed by Radok (1973).

It should be reemphasized that the model simulation results presented here represent ideal katabatic wind conditions with no clouds present to reduce the outgoing longwave radiation. Also, the two-dimensionality of the model presumes the y-variations (contour parallel) are not important. This is not entirely correct. The Antarctic continent is a dome of ice; slope-flows over the ice cap move outwards in a diffluent radial drainage pattern as shown in Parish (1982a). This spreading out of the flow away from the central ice plateau implies from mass continuity that a downward directed mass flux into the katabatic stream is necessary. This process cannot be simulated in a two-dimensional model. However, this subsidence effect is probably only of secondary importance owing to the large size of the continent and correspondingly weak radial diffluence and should not significantly alter the diagnostic analyses presented earlier. The same cannot be said for horizontal irregularities in the ice terrain contours. In particular, Parish (1984) has shown that wave-like variations in the ice topography force radical changes in the drainage patterns, creating marked confluent and diffluent regions. It has been proposed that such confluent patterns are responsible for significant enhancement of the katabatic winds downslope from the axis of confluence. Such drainage irregularities significantly influence the degree of entrainment into the katabatic layer. The confluence of cold air in the interior provides a large supply reservoir of negatively buoyant air available to feed downstream coastal stretches. The required downward transport of warmer, neutrally buoyant air from the free atmosphere into the katabatic stream is reduced by an amount depending on the degree of confluence. Conversely, diffluence requires an additional downward transport of mass into the katabatic stream. It is clear that such confluent/diffluent effects can significantly modulate the intensity of katabatic winds.

REFERENCES

Adachi, T., 1984: Numerical simulation of katabatic wind at Mizuho Station. *Me. Natl. Inst. Polar Res.*, Spec. Issue, **34,** 37–53. [Available from National Institute of Polar Research, Tokyo, Japan].

Anthes, R. A., and T. T. Warner, 1978: The development of hydrodynamic models suitable for air pollution and other mesometeorological studies. *Mon. Wea. Rev.*, **106,** 1045–1078.

Ball, F. K., 1960: Winds on the ice slopes of Antarctica. *Antarctic Meteorology, Proceedings of the Symposium,* Melbourne, 1959, Pergamon Press, 9–16.

Blackadar, A. K., 1978: High resolution models of the planetary boundary layer. *Advances in Environmental and Scientific Engineering,* Vol. 1, Gordon and Breach, 51–85.

Brost, R. A., and J. C. Wyngaard, 1978: A model study of the stably-stratified planetary boundary layer. *J. Atmos. Sci.*, **35,** 1427–1440.

Businger, J. A., J. C. Wyngaard, Y. Izumi and E. F. Bradley, 1971: Flux-profile relationships in the atmospheric surface layer. *J. Atmos. Sci.*, **28,** 181–189.

Cerni, T. A., and T. R. Parish, 1984: A radiative model of the stable nocturnal boundary layer with application to the polar night. *J. Climate and Appl. Meteor.*, **23,** 1563–1572.

Drewry, D. J., 1983: The surface of the Antarctic ice sheet. Sheet 2 of *Antarctica: Glaciological and Geological Folio,* D. J. Drewry, Ed., Scott Polar Research Institute, Cambridge. [Scott Polar Research Institute, University of Cambridge, Lensfield Road, Cambridge CB21ER, UK7.]

Kuhn, M., H. H. Lettau and A. J. Riordan, 1977: Stability related wind spiraling in the lowest 32-m. Meteorological studies at Plateau Station, Antarctica, Pap. 7, *Antarctic Research Series.*, Vol. 25, Amer. Geophys. Union, 93–111.

Manins, P. C., and B. L. Sawford, 1979a: A model of katabatic winds. *J. Atmos. Sci.*, **36,** 619–630.

Manins, P. C., and B. L. Sawford, 1979b: Katabatic winds: A field case study. *Quart. J. Roy. Meteor. Soc.*, **105,** 1011–1025.

Manins, P. C., and B. L. Sawford, 1979: A model of katabatic winds. *J. Atmos. Sci.*, **36,** 619–630.

Mather, K. B., and G. S. Miller, 1966: Wind drainage off the high plateau of eastern Antarctica. *Nature,* **209,** 281–284.

Mawson, D., 1915: *The Home of the Blizzard,* William Heinemann Co., Vol. 1, 349 pp. Vol. 2, 338 pp.

Parish, T. R., 1982a: Surface airflow over East Antarctica. *Mon. Wea. Rev.*, **110,** 84–90.

——, 1982b: Barrier winds along the Sierra Nevada Mountains. *J. Appl. Meteor.*, **21,** 35–40.

——, 1984: A numerical study of strong katabatic winds over Antarctica. *Mon. Wea. Rev.*, **112,** 545–554.

Radok, U., 1973: On the energetics of surface winds over the Antarctic ice cap. *Energy fluxes over polar surfaces,* WMO Tech. Note No. 129, Geneva, Switzerland, pp. 69–100. [World Meteorological Organization, Case postale No. 5, CH-1211, Geneva 20, Switzerland.]

Schwerdtfeger, W., 1970: *The Climate of the Antarctic,* Vol. 14, S. Orvig, Ed., *World Survey of Climatology,* H. E. Landsberg, Ed., Elsevier, 253–355.

——, 1984: *Weather and Climate of the Antarctic,* Elsevier, 261 pp.

Wendler, G., and Y. Kodama, 1984: On the climate of Dome C, Antarctica, in relation to its geographic setting. *J. Climatol.*, **4,** 495–508.

Unauthenticated | Downloaded 06/13/21 12:38 AM UTC